5th International Conference on Experimental Fluid Mechanics ICEFM 2018 Munich
Munich, Germany, July 2-4, 2018

Direct measurement of skin friction using TSP data

Massimo Miozzi[1*], Alessandro Capone[1], Marco Costantini[2], Lorenzo Fratto[1], Christian Klein[2], Fabio Di Felice[1]

[1] CNR-INM (formerly INSEAN), Marine Technology Institute of National Research Council / Rome / Italy

[2] DLR (German Aerospace Center) / Göttingen / Germany

[*] massimo.miozzi@cnr.it

Abstract

We provide a *proof-of-concept* about the direct measurement of skin friction τ by means of a Temperature-Sensitive Paint (TSP). To this aim, the relationships between the time-resolved measure of the surface temperature $T_w(x,y,t)$ below a turbulent boundary layer and the span- and time-averaged streamwise friction velocity $u_\tau(x)$ is firstly assessed. Then, the focus is placed on the turbulent region after the Laminar Separation Bubble (LSB) which develops on the suction side of a NACA 0015 hydrofoil model, investigated experimentally at chord Reynolds number $Re = 1.8 \times 10^5$ and angle of attack $AoA = 10°$. At spatial scales of the order of the LSB width, almost steady thermal footprints $T_w(x,y,t)$ of the fluid, slowly evolving around their averaged position, unveil a flow regime subject to small 2D disturbances. The LSB-induced spatial gradients of $T_w(x,y,t)$ are linked to almost fixed positions in time and any evidence of three-dimensional disturbance is missing. At smaller spatial scales, the legs of the turbulent structures rubbing the surface (hairpin vortexes) impress their thermal footprint on the TSP while they propagate in the streamwise direction. They act like a tracer and their strong preferential streamwise orientation suggests the application of a two-points cross-correlation algorithm, whose maximum provides the time-lag Δt between the appearance of a disturbance at the two streamwise aligned locations, and thus the propagation velocity u_{pT} of the T_w perturbation T_w'. The relationship between u_{pT} and the friction velocity u_τ feeds a physics-based criterion for the identification of span- and time-averaged separation x_S and reattachment x_R locations grounded on the sign of u_τ (and τ) itself. In the paper we report:

- The relationship between the velocity of propagation of the velocity disturbances u_{pU} and the friction velocity u_τ
- The relationship between the velocity of propagation of the temperature disturbances u_{pT} and u_{pU}
- The algorithm for the extraction of the propagation velocity of temperature perturbations u_{pT}
- The resulting friction velocity u_τ and friction coefficient C_f profiles.

1 Introduction

The measurement of the skin friction τ is a topic of great interest in various disciplines. The knowledge of τ and of the skin friction coefficient $C_f = \tau/0.5\rho U_\infty^2$, where ρ is the fluid density and U_∞ is the freestream velocity, is essential for the determination of the shear force that a flow acts on a body surface. It is also a primary scaling parameter for the theoretical treatment of wall turbulence, often via the friction velocity $u_\tau = \sqrt{\tau/\rho}$ (Tropea et al. (2007)). Moreover, the availability of time-resolved maps of skin friction vector fields enables a physics-based description of the wall-bounded flow in terms of separation, reattachment and laminar/turbulent transition (Hirschel et al. (2014)). Here we deal with this subject via an experimental approach whose focus is on the skin-friction data derived from time histories of temperature maps obtained using Temperature Sensitive Paint (TSP), see Tropea et al. (2007) for a description of the basic principles of this measurement technique. These maps retain a detailed portrait of the footprints of the coherent flow structures close to the surface, in a way that disregard the rigid hypothesis that the wall heat flux is only due

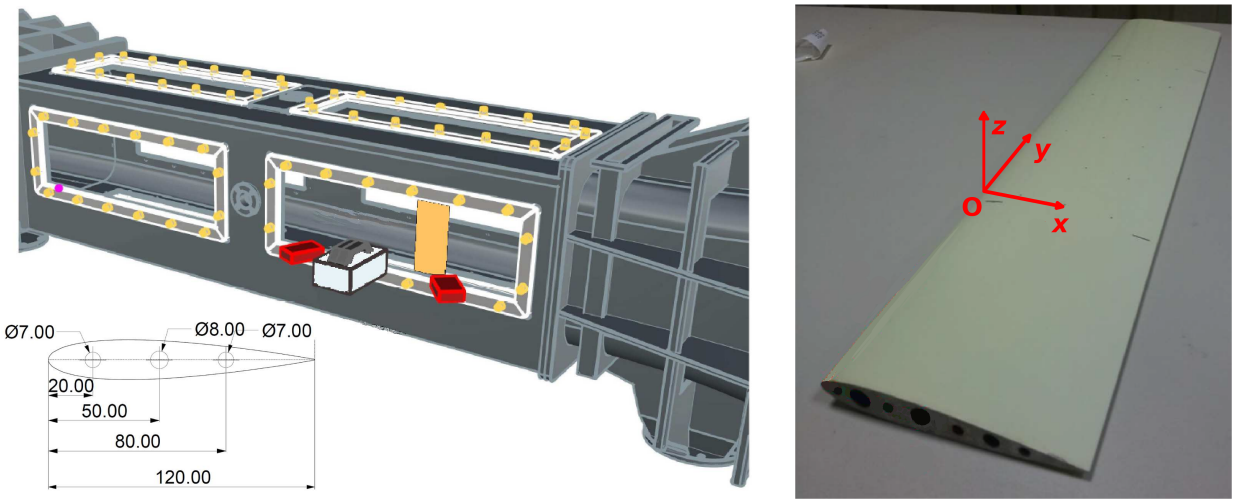

(a) CEIMM tunnel (b) TSP coated profile

Figure 1: (a) Water tunnel experimental setup and NACA 0015 hydrofoil model (orange, inside the tunnel), LED lamps (red) and fast camera (white). Lower left detail reports the NACA 0015 profile with heating structure. (b) TSP-coated hydrofoil model. Registration markers can be noticed onto the surface. Reference coordinates given (distances in mm).

to the convective action of the flow. We hypothesize that the temperature fluctuations T'_w, measured at the wall by means of TSP, can be used as tracers, so that their passages at close (but well separated), streamwise-aligned locations can be captured by a two-points correlation algorithm. The time lag corresponding to the maximum of the resulting correlation function allows for the calculation of a velocity which quantitatively describes the propagation of the temperature disturbances at wall, i.e. it provides a direct link to the friction velocity (Hetsroni et al. (2004)) and friction coefficient. This approach is well settled in literature for the speed of propagation of velocity and vorticity perturbations (see Kim and Hussain (1993)). Its extension to the T'_w propagation velocity u_{pT} in a turbulent channel establishes a proportionality with u_τ via a constant factor which is a function of the Prandtl (Pr) number and of the thermal boundary conditions (constant wall heat flux or wall temperature). It can be considered as a *ground-truth* reference in the turbulent channel literature. The present approach is feed by kinematic quantities and is not exposed to the influence of factors not related to fluid dynamic phenomena, such a non-uniform heating of the model needed for TSP (Tropea et al. (2007)).

2 Experimental setup

The cavitation tunnel CEIMM at CNR-INM (Rome) consists of a closed-loop water tunnel featuring a $1:5.96$ contraction nozzle and a square test section of side $B = 600\,\text{mm}$. Free-stream turbulence intensity and flow uniformity at the channel centerline are respectively 0.6% at hydrofoil position (1.5% on average) and 1%. The test section is bounded by perspex windows in order to allow optical access from all directions. The hydrofoil model cross-section is a NACA 0015, chord length $C = 120\,\text{mm}$ and length L equal to test section side B. The model was coated with a temperature-sensitive paint (TSP) to measure the surface temperature. The development and the properties of the TSP used in this work are described in Ondrus et al. (2015). The hydrofoil model, as shown in Fig. 1(b), is mounted at the channel centerline by means of two flanges which can be rotated to set the desired angle of attack. The images were acquired by a CMOS high-speed camera Photron Fastcam SAX, 1024 square pixels resolution, fitted with a Nikon 50 mm focal length lens with 1.4 maximum aperture and a long-wave pass filter having a 50% transmittance cut-point at 600 nm wave length. TSP coating excitation light is provided by twelve high-power LED devices, having their maxima in the wavelength range between 400 nm and 405 nm. Acquisitions were carried out at free-stream velocity $U = 1.5\,\text{m/s}$ corresponding to Reynolds number $Re = 1.8 \times 10^5$ based on chord length, and at angle of attack $AoA = 10°$. A set of 10,916 images was collected with acquisition frequencies of $F = 1\,\text{KHz}$. Imaged area for all acquisitions was approximately $135 \times 135\ mm^2$, thus image spatial resolu-

tion is $\approx 0.13\,\mathrm{mm/pixel}$. In order to establish a heat flux between the hydrofoil model surface and water, a temperature gradient has to be artificially created between the model profile and the surrounding fluid. To this aim the hydrofoil model was manufactured with three internal circular cavities having different diameters (7, 8 and 7 mm, positioned respectively at 20, 50 and 80 mm from the leading edge, see Fig. 1(a) (detail at lower left), through which warm water flows. This is supplied by an external thermostatic bath which keeps the inner-fluid temperature constant at a target value, about 15° higher than the free stream temperature T_∞. After reached, the target temperature was kept by the thermostatic bath for a long time (more than 5 min) before the experiment started. Then, the short duration of the tests (10 s) allows to consider the target temperature as a constant in that time lapse.
In order to assess the extent of natural convection effects, the Richardson non-dimensional number is calculated as:

$$Ri = (g\beta(T_W - T_\infty)L)/U^2 \tag{1}$$

which represents the importance of natural convection relative to forced convection with β representing the volumetric thermal expansion coefficient and T_W the hydrofoil model surface temperature. Typically, it is assumed that natural convection is negligible until $Ri < 0.1$. It follows that at the tested Reynolds number and angle of attack $Ri < 0.001$ holds and consequently natural convection can be reasonably deemed negligible.

2.1 Pre-processing methods

2.1.1 Temperature maps extraction

The acquired images were pre-processed according to the common practice adopted generally when dealing with TSP acquisitions. A detailed description can be found in Fey et al. (2003) and Capone et al. (2015) among the others. The aim of the procedure is to minimize the effect of non-uniform illumination, uneven coating and non-homogeneous luminophore concentration in the TSP active layer (Liu and Sullivan (2005)). In the presented experiments the hydrofoil model underwent a certain amount of displacement due to lift, this causing the reference and run images to mismatch. An image re-alignment step (image registration) was then necessary prior to the pixel-wise ratio calculation step. Based on reference markers printed onto the TSP coating, visible in Fig. 1(b), an affine geometric transformation was thus employed to re-align images. The ratioed images were converted to thermal maps by using an appropriate calibration curve (Capone et al. (2015)).

2.1.2 Spatial filtering

Although uneven paint coating and nonuniform surface illumination can be significantly reduced by following the procedure described in Sec. 2.1.1, TSP images are still affected by a signification amount of Gaussian, additive, white noise and a filtering is strongly suggested. With the aim to improve the efficiency of the classical Gaussian filter, an edge-preserving spatial filtering was developed in order to enhance the relevant image gradients in TSP images, while removing the background, uncorrelated noise. The proposed filter is an enhanced version of the classical Gaussian blur: a circular Gaussian kernel is applied to the image where where the luminosity gradients are negligible, whereas a weakly stretched Gaussian kernel in the direction normal to the gradient itself is applied to the image where it exhibits a spatially coherent gradient, thus preserving the gradient itself from smoothing (see Miozzi et al. (2018)).

2.1.3 Temporal filtering

Data are filtered in time with a Savitzky-Golay filter. It can be thought as a generalized moving average, which approximates the underlying function within the moving window by a polynomial of higher order. The filter was applied to each pixel's luminosity time series, with a polynomial order of 1 and a span of $2M+1 = 13$, where M is the impulse-response half length Schafer (2011). This corresponds to a nominal normalized cutoff frequency $f_{nc} = 0.165$ (Schafer (2011)), where the transfer function is 3 dB. The dimensional cutoff frequency of the filtered dataset is $f_c = 0.5 \times 0.165 \times 1000 = 82.5\,\mathrm{Hz}$.

3 Propagation velocity of fluid dynamic disturbances at the wall

The experimental evidence reported by Eckelmann (1974) about the direct relationship between u_τ and u_{pU} was obtained by comparing the fluctuations of the wall-normal gradient at wall $(\partial u(z,t)/\partial z)_w$ with the

horizontal velocity fluctuations $u'(z,t)$ acquired at increasing distances from the wall. He found an overall coincidence between the time dependency of the two profiles close to the wall in the range $0 < z^+ < 7$ (where $^+$ indicate an adimensional distance, defined as $z^+ = z \times u_\tau/\nu_\infty$ where ν_∞ the dynamic viscosity in free stream), being the two quantities scaled by a constant factor. The numerical investigation about the velocity of propagation of velocity disturbances $u_{pU}(z)$ as a function of the distance from the wall z (and its non dimensional counterpart z^+) in a turbulent channel flow by Kim and Hussain (1993) outlines how $u_{pU}(z)$ is slightly lower than the local mean flow velocity, except in the near wall region. For $z^+ < 5$, u_{pU} is essentially constant and greater than the local mean velocity, implying that *perturbation of fluid dynamic variables propagate like waves near the wall*. Their results are in good agreement with the numerical findings of Geng et al. (2015), among the others. The propagation of perturbances of T_w was considered by Hetsroni et al. (2004). They considered the influence on u_{pT} of the Prandtl number and of the boundary conditions in a turbulent flume and their findings confirm the existence of a region of constant u_{pT} below $z^+ = 2$, where two well-defined relationships hold, one at constant wall heat flux ($u^+_{pT} = Pr^{-1/2}u^+_p$) and the other at constant wall temperature ($u^+_{pT} = Pr^{-1/3}u^+_p$). By closing the circle with the findings of Eckelmann (1974), these relationships state that u_{pT} is also proportional to the friction velocity u_τ. Results about the streamwise component of u_{pT} will be shown in Sec. 4 in terms of u_τ and of the friction coefficient

$$C_f = \frac{\tau_w}{0.5\rho U^2_\infty} = 2\left(\frac{u_\tau}{u_\infty}\right)^2 = 2\left(\frac{u_{pT}/c}{u_\infty}\right)^2 \tag{2}$$

where $c = Pr^{-1/3}c_u$ is the constant of proportionality at constant wall temperature, $Pr = 7.56$ is the Prandtl number in water and $c_u = u_{pU}/u_\tau$ is the constant of proportionality between u_{pU} and the friction velocity u_τ after Kim and Hussain (1993) (see Miozzi et al. (2018)).
In contrast to the pressure transducers, which capture a non-localized quantity, results from Hetsroni et al. (2004) show how a measurement of u_{pT} at the wall is only related to the T_w values at $z^+ < 2$, where the u_{pT} distribution is constant. This property emphasizes the local nature of the TSP response, which excludes from the resulting signal statistics and spectra the occurrence of events localized at $z^+ > 2$, such as the Kelvin-Helmoltz induced vortex shedding and detachment in the shear layer of a laminar separation bubble (except for their impingement after the reattachment, see Miozzi et al. (2018)). Note that a similar analysis can be done also for laminar and transitional regions, as discussed in Miozzi et al. (2018).

4 Skin friction evaluation

Figures 2(a) and 2(b) report a snapshot of T and its detail at $AoA = 10°$. The whole snapshot of T'_w shows on the left the signature of the LSB, which is known to be almost steady at the inquired *Re* and *AoA* (Miozzi et al. (2018)). On the other hand, the elongated streaks of hotter and colder spots in Fig. 2(b) propagate streamwise at velocity u_{pT}. A criterion to quantitatively diagnostic the streamwise profile (x) of the time-averaged friction velocity u_τ and the related C_f profile is proposed as follows. Firstly, the best correlation distance $\Delta t_{max}(x,y)$ (time lag) is identified between temperature time-histories acquired simultaneously at adjacent, streamwise aligned, locations separated by $\Delta x \approx 1.3$ mm on average:

$$\Delta t_{max}(x,y)|\mathbb{R}^{\Delta x}_{TT}(x,y,\Delta t)|_{max} = \frac{\overline{T_w(x+\Delta x/2,y,t)\cdot T_w(x-\Delta x/2,y,t-\Delta t)}}{\sigma_{T(x_1,y)}\sigma_{T(x_2,y)}}|_{max} \tag{3}$$

where $\sigma_T(x,y)$ is the standard deviation of the temperature profile at (x,y):

$$\sigma_T(x,y) = \sqrt{\frac{1}{\mathsf{T}}\left(\sum_{t=1}^{\mathsf{T}}(T_w(x,y,t) - \langle T_w(x,y)\rangle_\mathsf{T})\right)^2} \tag{4}$$

where T is the time-length of T_w.

A propagation velocity at wall-normal distance z, $u_{pT}(z)|_{z\to 0}$, is then estimated as the ratio between the (curvilinear) locations separation in space and the identified time lag; eventually the friction velocity is calculated as $u_\tau = u_{pT}/c$. Results about u_τ are reported in Fig. 3(a), together with the 95% confidence interval.

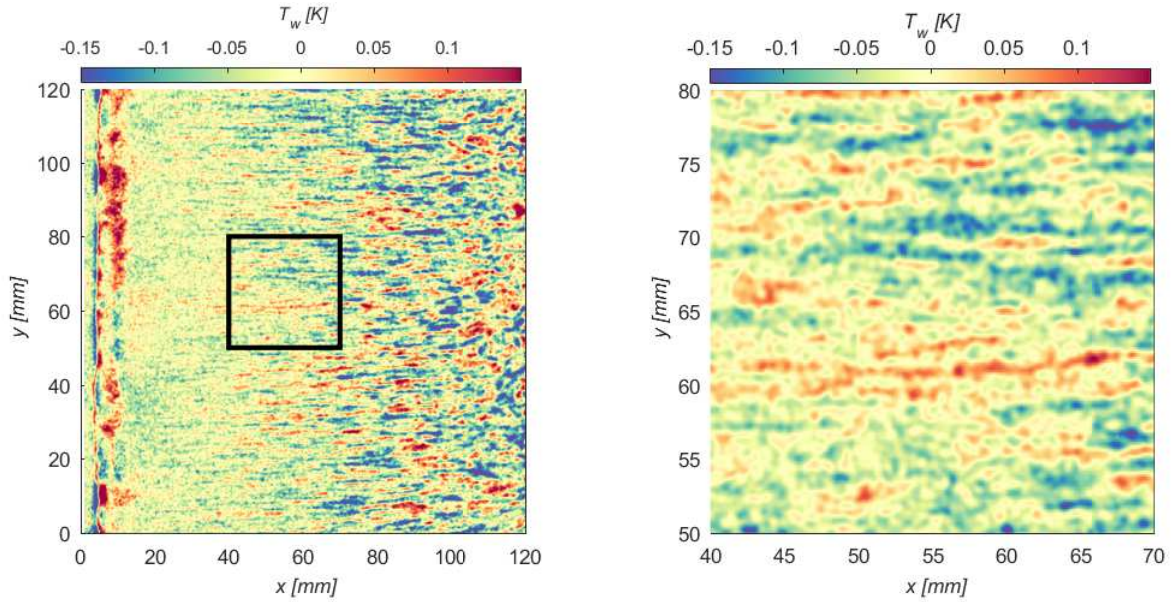

(a) Instantaneous T'_w map. LSB is visible on the left at $3 \leq x \leq 13$ mm.

(b) Detail of T'_w in the black square of Fig. 2(a)

Figure 2: Snapshot of T'_w at $AoA = 10^\circ$ (a) and its detail inside the black square (b). The thermal traces that move streamwise can be tracked by a classical correlation approach.

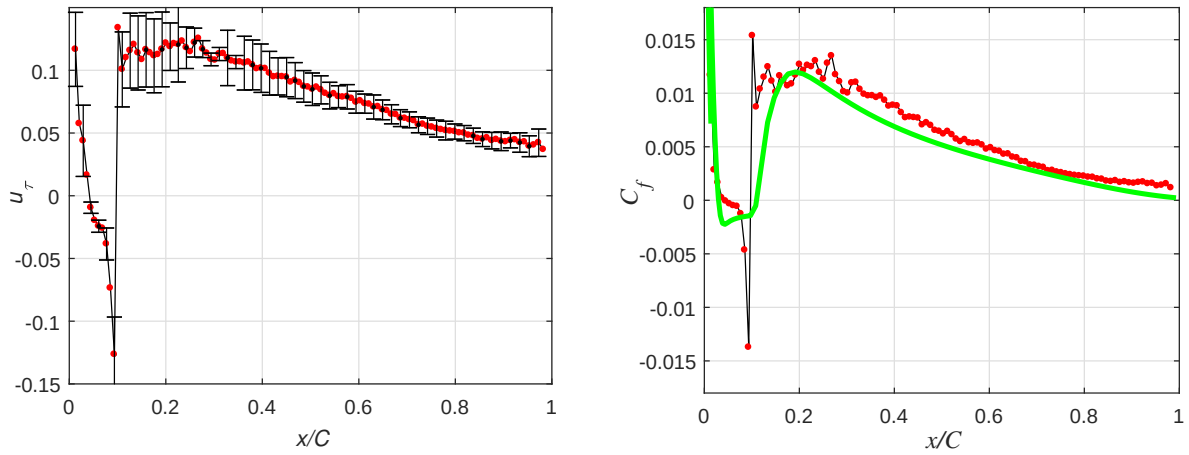

(a) u_τ profile (black line, calculated at red dots). Error bars report the 95% confidence interval.

(b) C_f profile from u_τ of Fig. 2(a) (black line, calculated at red dots) with results from Xfoil at $N_{crit} = 3.5$ (green line).

Figure 3: Span and time averaged profiles of u_τ (a) and C_f at $AoA = 10^\circ$ and $Re = 1.8 \times 10^5$. Error bars report the 95% confidence interval. Recirculating region is clearly detectable, together with the dead water region. The experimental C_f distributions is compared with Xfoil results in (b).

The profile of C_f, obtained following Eq. 2, is shown in Fig. 3(b). The existence of a reverse flow region is clearly visible and the separation and reattachment locations are immediately identifiable by looking at the change of sign of u_τ. The profile of C_f in Fig. 3(b) has been compared, in the same figure, with a profile obtained using Xfoil (Drela (1989)). Having in mind all the limits of the Xfoil implementation, especially for what concerns the value of the critical N-factor for transition N_{crit}, results obtained by placing $N_{crit} = 3.5$ (incoming turbulence level $T_u \approx 0.6\%$, see Xfoil documentation) show a meaningful correspondence, except inside the LSB, where the discrepancy is probably due to the limits in the Xfoil approach.

5 Conclusion

We report about the feasibility of the tracking of the temperature disturbances *at-wall* for the quantitative estimation of the friction velocity u_τ. The method, fed with results from surface temperature measured by means of TSP, relies on kinematic properties of temperature signals and is not affected by non uniform heating of the model. This *proof-of-concept* is developed on the turbulent region downstream the almost steady LSB on the suction side of a NACA0015 hydrofoil model at $AoA = 10^\circ$ and demonstrates the capabilities of the approach in the challenging occurrence of a LSB. The ubiquity of the turbulence tracers guarantees an accurate seeding of the investigated surface, while more refined correlation strategies are required to overcome the weak signal-to-noise ratio. By stating the relationship between u_{pT} and u_τ and by considering the analogy between the flow turbulence at wall (i.e. thermal traces of hairpin vortexes legs) and flow seeding in the fluid we can consider the present approach as a PIV-like investigation of the flow at the wall, i.e. a Wall-Turbulence Image Velocimetry.

Acknowledgements

This work has been supported by the Flagship Project RITMARE, The Italian Research for the Sea, coordinated by the Italian National Research Council and funded by the Italian Ministry of Education, University and Research. Carsten Fuchs (DLR) is acknowledged for TSP surface treatment.

References

Capone A, Klein C, Di Felice F, Beifuss U, and Miozzi M (2015) Fast-response underwater TSP investigation of subcritical instabilities of a cylinder in crossflow. *Experiments in Fluids* 56:1–14

Drela M (1989) Xfoil: An analysis and design system for low reynolds number airfoils. in TJ Mueller, editor, *Low Reynolds Number Aerodynamics*. pages 1–12. Springer Berlin Heidelberg, Berlin, Heidelberg

Eckelmann H (1974) The structure of the viscous sublayer and the adjacent wall region in a turbulent channel flow. *Journal of Fluid Mechanics* 65:439–459

Fey U, Engler R, Egami Y, Iijima Y, Asai K, Jansen U, and Quest J (2003) Transition detection by temperature sensitive paint at cryogenic temperatures in the european transonic wind tunnel (etw). in *ICIASF Record, International Congress on Instrumentation in Aerospace Simulation Facilities*. pages 77–88

Geng C, He G, Wang Y, Xu C, Lozano-Durán A, and Wallace JM (2015) Taylor's hypothesis in turbulent channel flow considered using a transport equation analysis. *Physics of Fluids* 27:025111

Hetsroni G, Tiselj I, Bergant R, Mosyak A, and Pogrebnyak E (2004) Convection velocity of temperature fluctuations in a turbulent flume. *Journal of Heat Transfer* 126:843–848

Hirschel E, Kordulla W, and Cousteix J (2014) *Three-dimensional attached viscous flow: Basic principles and theoretical foundations*. Springer

Kim J and Hussain F (1993) Propagation velocity of perturbations in turbulent channel flow. *Physics of Fluids A* 5:695–706

Liu T and Sullivan JP (2005) *Pressure-and Temperature-Sensitive Paints*. Wiley Online Library

Miozzi M, Capone A, Costantini M, Fratto L, Klein C, and Di Felice F (2018) Skin friction and coherent structures within a laminar separation bubble. Submitted to Experiments in Fluids

Ondrus V, Meier R, Klein C, Henne U, Schäferling M, and Beifuss U (2015) Europium 1,3-di(thienyl)propane-1,3-diones with outstanding properties for temperature sensing. *Sensors and Actuators A: Physical* 233:434 – 441

Schafer RW (2011) What is a Savitzky-Golay filter?. *IEEE Signal Processing Magazine* 28:111–117

Tropea C, Yarin AL, and Foss JF (2007) *Springer handbook of experimental fluid mechanics*. volume 1. Springer Science & Business Media